Inorganic Chemistry

Article

pubs.acs.org/IC

Thiacalix[4]arene-Supported Kite-Like Heterometallic Tetranuclear $Zn^{II}Ln^{III}_3$ (Ln = Gd, Tb, Dy, Ho) Complexes

Kongzhao Su,[†,‡] Feilong Jiang,[†] Jinjie Qian,[†,‡] Mingyan Wu,[†] Kecai Xiong,[†,‡] Yanli Gai,[†,‡] and Maochun Hong*[,†]

[†]Key Laboratory of Optoelectronic Materials Chemistry and Physics, Fujian Institute of Research on the Structure of Matter, Chinese Academy of Sciences, Fuzhou, 350002, China

[‡]Graduate School of the Chinese Academy of Sciences, Beijing, 100049, China

Supporting Information

ABSTRACT: Four kite-like tetranuclear $Zn^{II}Ln^{III}_3$ (Ln= Gd **1**, Tb **2**, Dy **3**, Ho **4**) clusters supported by *p-tert*-butylthiacalix[4]arene (H_4BTC4A) have been prepared under solvothermal conditions and structurally characterized by single crystal X-ray diffraction and powder X-ray diffraction (PXRD). In the structures of these four complexes, each of them is capped by two tail-to-tail *p-tert*-butylthiacalix[4]arene molecules to form a bent sandwich-like unit. The photoluminescent analyses reveal that the H_4BTC4A is an efficient sensitizer for Tb^{3+} ions in **2**. The magnetic properties of complexes **1**−**4** are also investigated, in which complex **3** exhibits slow magnetization relaxation typical for single molecule magnets.

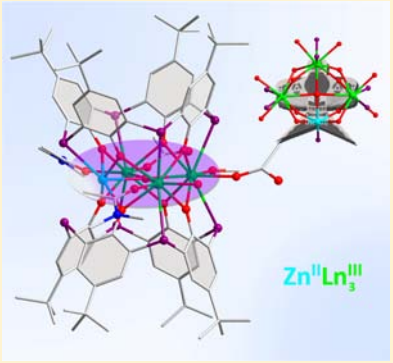

INTRODUCTION

The development of methods for preparing transition−lanthanide (3d-4f) heteropolynuclear complexes has attracted extensive attention in recent decades, not only because of their novel structural architectures and topologies[1] but also because of their potential applications in gas adsorption and storage,[2] catalysis,[3] magnetism,[4] and optical properties.[5] The recent increasing interest is refocused on the synthesis of lanthanide-based polymetallic clusters, because they exhibit strong spin−orbital coupling and, in some cases, strong anisotropic easy-axis,[6] which might be helpful in building single-molecule magnets (SMMs),[4a−c] single chain magnets (SCMs),[4d] and magnetic refrigerants,[4e,f] and which also makes the magnetic properties of 3d-4f heterometallic complexes significantly different from those of homometallic 3d ones. Indeed, this approach has successfully led to several 3d-4f functional magnetic materials.[7] As is widely known, lanthanide ions have not only high coordination number and flexible coordination geometry but also high affinity for organic ligands containing hard donor atoms, especially multidentate ligands, which usually are employed in the design and construction of lanthanide coordination clusters. On the other hand, direct transitions to the excited 4f levels of the Ln^{III} ions are spin and parity forbidden, while organic ligands can absorb light in the ultraviolet region and transfer the energy via the so-called "antenna effect" from excited states of the ligands to f-excited states; therefore those ligands are preferred in the architectures for luminescent materials. All in all, it is a critical factor to rationally select and synthesize organic ligands to prepare the multifunctional 3d-4f based materials.

More recently, to construct polymetallic complexes by using calixarenes is a research hotspot in the chemical community, where the calixarenes consisting of several phenolic groups are good candidates as versatile ligands.[8] A large number of polymetallic complexes based on alkali ions,[9] transition metals,[10] or lanthanide species[11] with calixarenes have been synthesized so far. What is more, thiacalixarenes, as macrocyclic π-rich ligands linked by sulfur bridges, have similar shapes and structures with calixarenes, which may lead to more efficient energy transfer properties for the luminescent materials and proper orbitals for the construction of transition-lanthanide magnetic materials. Many studies have indicated that thiacalixarenes are not simple substitutes for conventional calixarenes, which could be regarded as emerging and particular ligands in the calixarene chemistry. We note that the bridging sulfur here plays an important role in enlarging the calix skeleton to provide a larger cavity, makes the macrocycle more flexible, and is oxidized to sulfoxide and sulfone to provide new members of sulfur bridged calixarenes. Therefore, thiacalixarenes and their oxidized derivatives with additional donor atoms around the molecular skeletons have been used in the formation of many polymetallic complexes by taking part in bonding to the metal-cluster frameworks.[12]

Received: October 30, 2012
Published: March 13, 2013

   dx.doi.org/10.1021/ic302367q | *Inorg. Chem.* 2013, 52, 3780−3786

Table 1. Crystal Data and Data Collection and Refinement Parameters for 1−4

	1	2	3	4
formula	$C_{93}H_{121}N_2O_{20}S_8ZnGd_3$	$C_{93}H_{121}N_2O_{20}S_8ZnTb_3$	$C_{93}H_{121}N_2O_{20}S_8ZnDy_3$	$C_{93}H_{121}N_2O_{20}S_8ZnHo_3$
formula weight	2380.63	2385.66	2396.38	2403.67
temperature (K)	298 (2)	298 (2)	298 (2)	298(2)
wavelength (Å)	0.71073	0.71073	0.71073	0.71073
crystal system	monoclinic	monoclinic	monoclinic	monoclinic
space group	$P2_1/n$	$P2_1/n$	$P2_1/n$	$P2_1/n$
a (Å)	23.265 (7)	23.640 (6)	23.479 (9)	23.4538 (9)
b (Å)	12.925 (3)	13.045 (3)	12.952 (5)	12.9420 (3)
c (Å)	36.57 (1)	36.394 (9)	36.47 (1)	36.293(1)
α (deg)	90	90	90	90
β (deg)	100.366 (5)	100.914 (5)	100.740 (7)	100.780 (2)
γ (deg)	90	90	90	90
volume (Å^3)	10893 (7)	11021 (5)	10893 (7)	10821.5 (6)
Z	4	4	4	4
D_c (Mg/m^3)	1.4620	1.4376	1.4672	1.4751
μ (mm^{-1})	2.25	2.33	2.46	2.56
data collected	57976	53542	75875	44811
unique data (R_{int})	18466	18883	24550	17664
parameters	1202	1148	1182	1162
GOF on F^2	1.096	1.037	1.099	1.074
$R_1{}^a$ [$I > 2(I)$]	0.0778	0.0872	0.0857	0.0497
$wR_2{}^b$	0.2068	0.3474	0.2324	0.1420

$^a R_1 = \sum||F_o| - |F_c||/\sum|F_o|$. $^b wR_2 = \{\sum[w(F_o^2 - F_c^2)^2]/\sum[w(F_o^2)^2]\}^{1/2}$.

In spite of the fact that calixarenes make it facile to construct polymetallic complexes, there are few reports on calixarene-supported 3d-4f mixed-metal clusters. To our best knowledge, these polynuclear 3d-4f heterometallic complexes sustained by calixarenes reported so far all contain an even number of transition ions and an even number of lanthanide metal ions, for instance, our group reported two $Ni^{II}_{12}Ln^{III}_2$ clusters with H_4BTC4A,[13a] Dalgarno and co-workers obtained three $Mn^{III}_4Ln^{III}_4$ calix[4]arene clusters as enhanced magnetic coolers and molecular magnets[4f,g] and three calix[4]arene-supported $Fe^{III}_2Ln^{III}_2$ clusters,[13b] the group of Liao prepared a $Mn^{II}_2Gd^{III}_2$ cluster with H_4BTC4A, and two $Mn^{II}_2Ln^{III}_4$ complexes of *p-tert*-butylsulfinylcalix[4]arene.[13c,d] On the other hand, there are no reports on calixarene-supported Zn/Ln 3d-4f heterometallic clusters to date. In this work, we have successfully synthesized four 3d-4f heterometallic clusters with one zinc ion and three lanthanide ions, namely, $[Zn^{II}Ln^{III}_3(\mu_4\text{-}OH)(BTC4A)_2(OAc)_2(CH_3OH)(H_2O)(DMA)_2]\cdot 3H_2O$ (Ln= Gd (**1**), Tb (**2**), Dy (**3**), Ho (**4**); H_4BTC4A= *p-tert*-butylthiacalix[4]arene, HOAc = CH_3CO_2H, DMA= *N,N′*-dimethylacetamide). Herein, the syntheses, structures, luminescent and magnetic properties of complexes **1**−**4** are presented and discussed.

EXPERIMENTAL SECTION

Materials and Measurements. *p-tert*-Butylthiacalix[4]arene was prepared as reported in the literature,[14] and other chemicals were of reagent grade quality purchased from commercial sources and used as received. Elemental analyses were performed with a German Elementary Varil EL III instrument. IR spectra were recorded in the range 4000−400 cm^{-1} with a Magna 750 FT-IR spectrometer using KBr pellets. Metal elemental analysis was determined by an Ultima-2 ICP Emission Spectrometer. The powder X-ray diffraction (PXRD) were recorded by a RIGAKU-DMAX2500 X-ray diffractometer using Cu Kα radiation (λ = 0.154 nm) at a scanning rate of 3°/min for 2θ ranging from 2° to 50°. Thermogravimetric analysis (TGA) was performed using a NETZSCH STA 449C instrument. Samples and reference (Al_2O_3) were enclosed in a platinum crucible and heated at a rate of 10 °C/min from room temperature to 1000 °C under nitrogen atmosphere. Emission spectra were measured at 293 K with an Edinburgh FL-FS90 TCSPC system. Magnetic susceptibilities were carried out on a Quantum Design PPMS-9T and MPMS-XL systems in the range of 2−300 K.

Syntheses of Complexes 1−4. In a general procedure, a mixture of H_4BTC4A·$CHCl_3$ (0.12 mmol, 82 mg), $Zn(OAc)_2\cdot 2H_2O$ (0.46 mmol, 100 mg), and $Ln(OAc)_3\cdot 6H_2O$ (0.22 mmol, 100 mg) in DMA/CH_3OH (5/5 mL) was sealed in a 25 mL Teflon-lined bomb at 120 °C for 3 days and then cooled slowly at 4 °C h^{-1} to room temperature. Colorless prismatic crystals were isolated by filtration, washed with DMA/CH_3OH (1:1, v/v), and air-dried.

Complex 1. Yield 47% with respect to H_4BTC4A. Anal. Calcd. for complex **1**: calcd. C, 46.93; H, 5.12; N, 1.17. found C, 46.77; H, 5.09; N, 1.18. IR (KBr disk, ν cm^{-1}): 3416 (w), 2953 (s), 2896 (m), 2864 (m), 1619 (s), 1560 (m), 1443 (s), 1361 (m), 1312 (s), 1259 (s), 1199 (w), 1090 (w), 1024 (w), 886 (w), 837 (w), 748 (w), 621 (w), 543 (w).

Complex 2. Yield 53% with respect to H_4BTC4A. Anal. Calcd. for complex **2**: calcd. C, 46.82; H, 5.10; N, 1.17. found C, 46.64; H, 5.13; N.1.14. IR (KBr disk, ν cm^{-1}): 3416 (w), 2961 (s), 2899 (w), 2869 (w), 1613 (m), 1559 (m), 1435 (s), 1361 (w), 1307 (m), 1259 (s), 1096 (w), 1018 (w), 916 (w), 873 (w), 832 (m), 748 (w), 628 (w), 532 (w).

Complex 3. Yield 48% with respect to H_4BTC4A. Anal. Calcd. for complex **3**: calcd. C, 46.61; H, 5.09; N, 1.16. found C, 46.37; H, 5.12; N, 1.19. IR (KBr disk, ν cm^{-1}): 3422 (w), 2965 (s), 2899 (m), 2869 (m), 1613 (s), 1553 (m), 1445 (s), 1361 (m), 1312 (m), 1259 (s), 1199 (w), 1096 (w), 1024 (w), 916 (w), 880 (w), 831 (m), 742 (m), 622 (w), 538 (w).

Complex 4. Yield 56% with respect to H_4BTC4A. Anal. Calcd. for complex **4**: calcd. C, 46.47; H, 5.07; N, 1.16. found C, 46.34; H, 5.09; N, 1.15. IR (KBr disk, ν cm^{-1}): 3422 (w), 2959 (s), 2905 (m), 2856 (m), 1619 (s), 1457 (s), 1361 (m), 1312 (m), 1252 (s), 1090 (m), 1018 (m), 916 (w), 880 (w), 838 (m), 742(m), 628 (w), 538 (w).

X-ray Data Collection and Structure Determination. The X-ray intensity data for complexes **1**−**4** were collected on a Rigaku-CCD diffractometer equipped with graphite monochromated Mo−Kα radiation (λ = 0.71073 Å) by using the ω-scan mode at 298 K. All

dx.doi.org/10.1021/ic302367q | Inorg. Chem. 2013, 52, 3780−3786

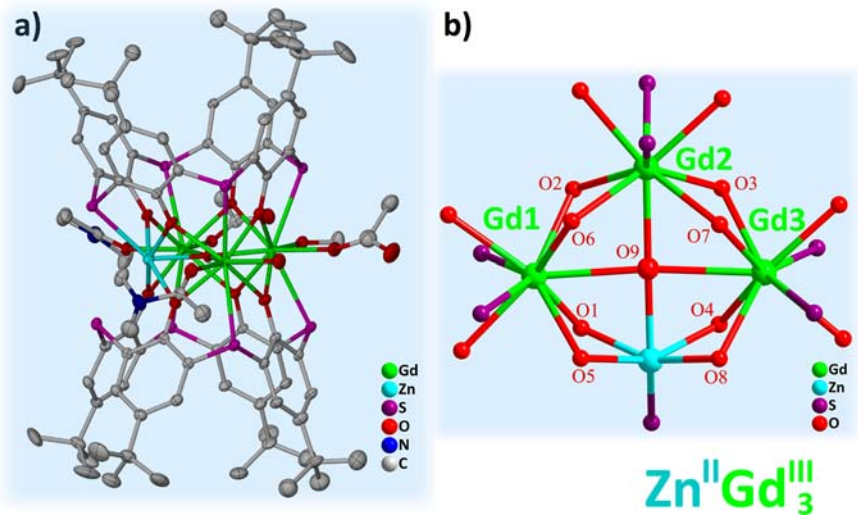

Figure 1. (a) Thermal ellipsoid (30% probability) plot of complex **1**. The hydrogen atoms and isolated solvent molecules are omitted for clarity. (b) The kite-like tetranuclear $Zn^{II}Gd^{III}_3$ core within complex **1**.

absorption corrections were applied using the CrystalClear program.[15] The crystal structures were solved by direct methods and refined using full-matrix least-squares on F^2 by the SHELXTL-97 program package.[16] All the non-hydrogen atoms were refined anisotropically except some badly disordered atoms and some solvent molecules. Hydrogen atoms of the organic ligands were generated theoretically onto the specific atoms and refined isotropically with fixed thermal factors. Hydrogen atoms on coordinated water and solvent molecules cannot be generated, but they were included in the molecular formula directly. Moreover, the high R_1 and wR_2 factor of complexes **1**–**4** might be due to the weak crystal diffractions and the disorder of the solvent molecules. Details of the structure solution and final refinements for these four complexes are given in Table 1. CCDC numbers 906782–906785 are for complexes **1**–**4**, respectively. These data can be obtained free of charge from The Cambridge Crystallographic Data Centre via www.ccdc.cam.ac.uk/-data_request/cif.

RESULTS AND DISCUSSION

Crystal Structures. Crystals of complexes **1**–**4** crystallize in the monoclinic space group $P2_1/n$. These four thiacalix[4]-arene-supported $Zn^{II}Ln^{III}_3$ (Ln= Gd **1**, Tb **2**, Dy **3**, Ho **4**) complexes are structurally analogous and show similarity in the coordination environment except for the slight differences in the bond lengths and angles, respectively. Here we only provide structure **1** as generic description. The essential feature of complex **1** possesses a sandwich-like unit composed of two tail-to-tail $BTC4A^{4-}$ ligands and a $Zn^{II}Ln^{III}_3$ square housing a central μ_4-OH^- ion, as can be seen from Figure 1a.

In the structure of complex **1**, there are four crystallographic sites for the metal ions (Zn, Gd1, Gd2, and Gd3), adopting a kite-like tetragonal Zn–Gd–Gd–Gd mode as shown in Figure 1b. The Zn^{II} site is six-coordinated in a seriously distorted octahederal coordination environment with four phenoxyl oxygen atoms, one sulfur atom, and one μ_4-OH^-, while each Gd^{III} ion is nine-coordinated in distorted tricapped trigonal prismatic geometry, coordinated by four phenoxyl oxygen atoms, two sulfur atoms, one μ_4-OH^-, and two other components (DMA and H_2O molecules for Gd1; CH_3OH molecule and OAc^- for Gd2; DMA molecule and OAc^- for Gd3). All phenoxyl oxygen atoms are connected to two metal ions to stabilize the tetragonal $Zn^{II}Ln^{III}_3$ arrangement, with Gd–$O_{phenoxyo}$–Gd and Zn–$O_{phenoxyo}$–Gd angles being in the range of 97.99–99.12° and 95.41–97.67°, respectively. Moreover, the neighboring Zn–Gd/Gd–Gd distances in the edge linked by $O_{phenoxyo}$ are 3.337/3.340 Å and 3.638/3.667 Å, respectively, while the diagonal metal distances linked by μ_4-OH^- are 4.576 and 5.270 Å, which looks like a kite. It should be pointed out that the central μ_4-OH^- (O9) ion adopts a little distorted square-planar geometry with Gd2–O9–Zn and Gd1–O9–Gd3 angles being of 177.32° and 173.76°, and Zn–O9, Gd–O9 distances being of 2.190 and 2.620/2.390/2.658 Å, respectively (Supporting Information, Table S1). Although there has been a report with a thiacalix[4]arene-supported tetragonal $Mn^{II}_2Gd^{III}_2$ cluster housing a similar geometrical μ_4-OH^- ion, those four metal ions form an isosceles trapezoid shape.[13c] Furthermore, the $Zn^{II}Ln^{III}_3$ square is surounded by two tail-to-tail thiacalix[4]arene ligands to form a bent sandwich-like unit with metal ions, which is different from those formed in the routine antiparallel arrangements found in the monometallic $BTC4A^{4-}$ sandwiches.[9a,11a] The formation of the bent sandwich-like unit might be attributed to the following two reasons: (i) thiacalix[4]arene with four bridging sulfur atoms is more flexibile than calix[4]arene, which can easily bind to different metal ions simultaneously forming metal-thiacalix[4]arene clusters; (ii) the radius of zinc atom is smaller than the radius of gadolinium atom in the tetragonal $Zn^{II}Ln^{III}_3$ unit, which would lead the thiacalixarene molecules to be more inclined to the zinc side. It should be noticed that comparing with the pure tetranuclear Ln_4 clusters supported by thiacalix[4]arene which was reported by the groups of Liao and Gao,[11a] one can observe a rough geometrical change in the binding pocket moving from approximate rhombus to kite-like shape. Therefore, it is indicated that we can modulate the degree of the bent sandwich-like units by supporting with $BTC4A^{4-}$ ligands and the distances between metal ions by changing the radius ratio of metal ions, which might influence the cluster composition and further influence the magnetic properties.

The extended structure of **1** is constructed by the stacking of the sandwich-like entities, which further assemble into a slightly skewed head-to-head bilayer array through van der Waals interactions, $\pi\cdots\pi$, C–H$\cdots\pi$ and H-bonding interactions (Figure 2). Furthermore, one water molecule penetrates into

dx.doi.org/10.1021/ic302367q | Inorg. Chem. 2013, 52, 3780–3786

the thiacalixarene cavity via two O−H···π interactions, and some solvent hydrate molecules occupy the crystal interstices.

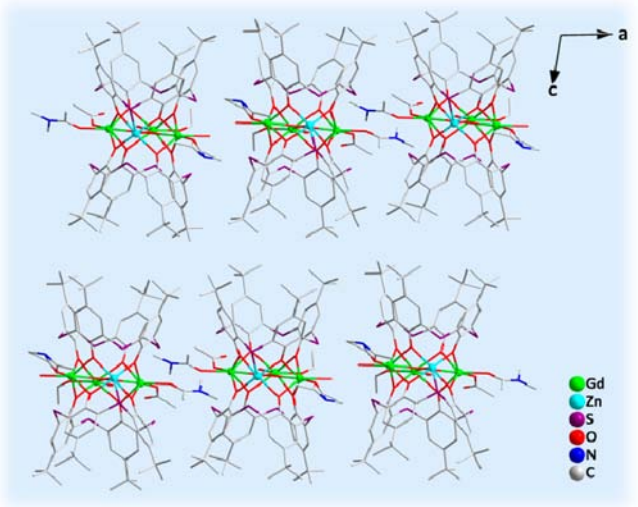

Figure 2. Extended structure of complex **1** showing self-assembly into a slightly skewed bilayer array. The hydrogen atoms and isolated solvent molecules are omitted for clarity.

Photoluminescent Properties. The solid-state excitation and emission spectra of complex **2** at room temperature are shown in Figure 3. The excitation spectrum is obtained by monitoring the 544 nm line of the strongest $^5D_4 \rightarrow {}^7F_5$ emission. The broad band between 250 and 400 nm for complex **2** can be assigned to the n,$\pi \rightarrow \pi^*$ electronic transition of the ligand, which mimics that of its corresponding ligand absorption spectrum. The absence of any typical absorptions of Tb^{3+} indicates that energy transfer from the ligand to the metal ion is effective. When excited at 350 nm (the ligand band), complex **2** shows an intense green luminescence and exhibits characteristic peaks at 489, 545, 586, and 620 nm originating from $^5D_4$ excited state to the corresponding ^7F_J ground state (J = 6, 5, 4, 3) of the Tb^{3+} cation. And the ligand fluorescence disappears completely, further revealing that luminescence sensitization of the Tb^{3+} complex via excitation of the ligand is efficient. Lifetime measurement at room temperature provides the decay process of the $^5D_4$ luminescence of Tb^{3+} (excited at 350 nm). The decay curve is well-produced by a double-exponential function with decay times τ_1 being 1.09 ms (93.26%) and τ_2 being 0.25 ms (6.14%). The emission quantum yield ($\Phi_{overall}$) is 29.80% at room temperature under the excitation wavelength 350 nm.

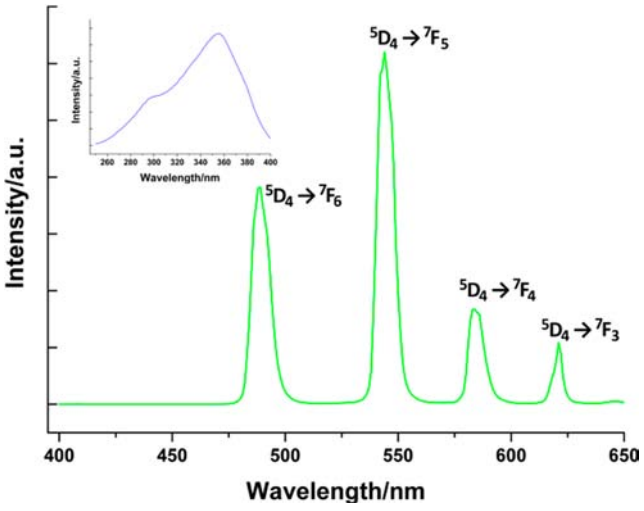

Figure 3. Room-temperature emission spectrum for complex **2** excited at 350 nm. Inset: Excitation spectrum of complex **2** monitored at 544 nm.

For complex **3**, the excitation spectrum exhibits a broad band from 250 to 400 nm, which belongs to the n,$\pi \rightarrow \pi^*$ energy transfer of the ligand (Figure 4). The presence of three sharp peaks ascribed to the characteristic absorptions of Dy^{3+} ion indicates that the ligand makes insignificant contributions to the corresponding complex. The ambient-temperature emission spectrum of **3** is measured in the 400−650 nm range under excitation at 365 nm. Three major peaks at 407, 479, and 572 nm are observed in the emission spectrum of **3**. The emission peaks at 479 and 572 nm are ascribed to the characteristic emission of Dy^{3+} corresponding to $^4F_{9/2} \rightarrow {}^6H_{15/2}$ and $^4F_{9/2} \rightarrow {}^6H_{13/2}$ transitions. The strongest emission band located at about 407 nm can be assigned to ligand fluorescence, also indicating that Dy^{3+} luminescence is not efficiently sensitized by the ligand. However, the lifetime and emission quantum yield of complex **3** are too weak to be measured with our instrument setup.

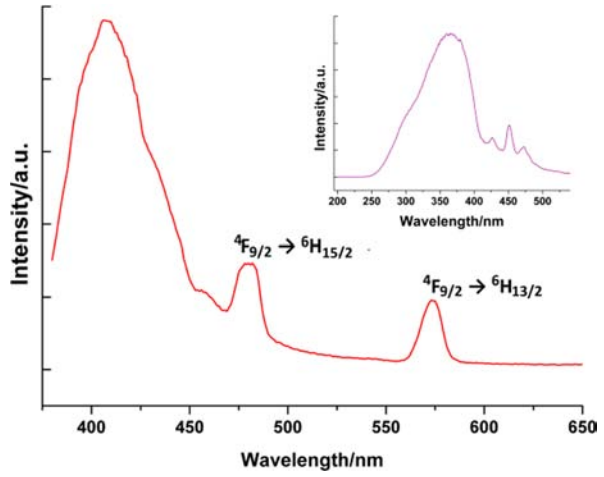

Figure 4. Room-temperature emission spectrum for complex **3** excited at 365 nm. Inset: Excitation spectrum of complex **3** monitored at 572 nm.

Magnetic Studies. The temperature dependence of magnetic susceptibility is performed on the polycrystalline samples of **1**−**4** in the 2−300 K range under an applied field of 1 kOe, as shown in Figure 5. The room temperature $\chi_m T$ are 23.13, 35.81, 41.12, and 39.23 cm^3 K mol^{-1} for complexes **1**−**4**, respectively, which are in agreement with the expected value of 23.64, 35.46, 42.51, and 42.21 cm^3 K mol^{-1} for three uncoupled Gd^{III} ($^8S_{7/2}$, S = 7/2, L = 0, g = 2), Tb^{III} ($^7F_6$, S = 3, L = 3, g = 3/2), Dy^{III} ($^6H_{15/2}$, S = 5/2, L = 5, g = 4/3), and Ho^{III} ($^8I_5$, S = 2, L = 6, g = 5/4) spin carriers. For complexes **1**−**3**, the $\chi_m T$ value remains roughly constant with decreasing temperature down to 50 K, and then drops dramatically to the minimum values of 11.80, 15.74, and 25.38 cm^3 K mol^{-1} at 2 K, respectively, while the $\chi_m T$ value gradually decreases and then falls rapidly to 8.02 cm^3 K mol^{-1} at 2 K for complex **4**. The abrupt decrease of the $\chi_m T$ curves at low temperature might

dx.doi.org/10.1021/ic302367q | Inorg. Chem. 2013, 52, 3780−3786

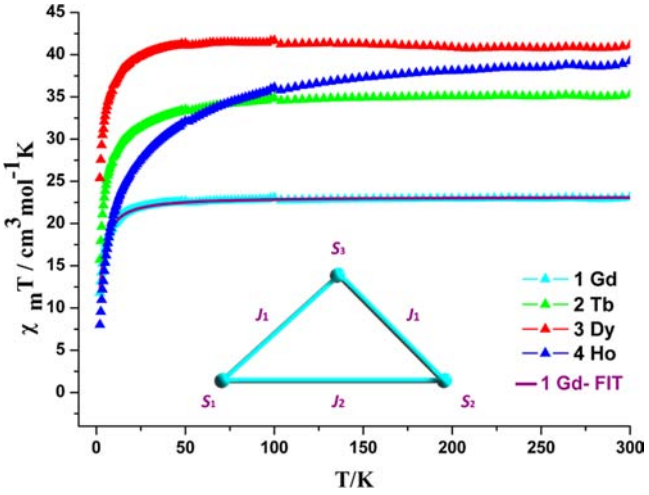

Figure 5. Temperature dependence of magnetic susceptibilities of **1**−**4** in a 1 kOe field. The solid line is a fit of the experimental data of **1** using the coupling scheme shown in the inset.

arise from the antiferromagnetic interaction between the lanthanide centers, although, except for complex **1**, the presence of significant magnetic anisotropy probably also causes the abrupt decrease.[17] In addition, the different magnetic behavior observed for **4** might be due to the orbital contribution induced by the thermal depopulation of the Stark sublevels of the anisotropic Ho ^{III} ions, which can be responsible for the decrease of the $\chi_m T$ value.[18]

Fitting the experimental data of **1** in the region of 2−300 K to the Curie−Weiss law gives the Curie constants C = 23.11 cm^3 mol^{-1} K and Weiss constants θ = −1.00 K, which indicates dominant antiferromagnetic interactions between spin carriers. The experimental $\chi_m T$ susceptibility data for complex **1** can be fitted with a Heisenberg−Dirac−Van Vleck model (eq 1), depicted in Figure 5 (inset). The best fit parameters obtained from fitting the $\chi_m T$ data are J_1 = −0.026 cm^{-1}, J_2 = −0.157 cm^{-1}, and g = 1.98 (Supporting Information, Equation S1). These data further suggest the intramolecular antiferromagnetic couplings in **1**.

$$\hat{H} = -2J_2\hat{S}_1\hat{S}_2 - 2J_1(\hat{S}_1\hat{S}_3 + \hat{S}_2\hat{S}_3) \quad (1)$$

To further reveal the dynamics of the magnetization which may originate from an SMM behavior, temperature dependent alternating current (*ac*) measurements are undertaken on all complexes in the temperature range 2−20 K with zero direct current (dc) field and a 3 Oe *ac* field. The *ac* susceptibilities of **3** show that both in- and out-of-phase susceptibilities are strongly frequency dependent below 10 K, and no peaks are displayed until 2 K (Figure 6). These phenomena suggest the $Zn^{II}Dy^{III}_3$ complex is a possible SMM, but one with a rather small barrier to magnetization reversal. Further confirmation of the SMM behavior has to measure magnetization versus dc field scans on single crystals employing a micro-SQUID. Moreover, complexes **1**, **2**, and **4** do not exhibit any frequency-dependent signals, which indicate no SMM behavior above 2 K (Supporting Information, Figures S1−S3).

Field-dependent magnetization $M(H)$ of **1**−**4** is investigated with the applied magnetic field H in the range 0−80 kOe at 2 K. Upon increasing the applied external magnetic field, complexes **1**−**4** show a rapid increase of the magnetization at low fields, and then reach the maximum values of 20.75, 24.33,

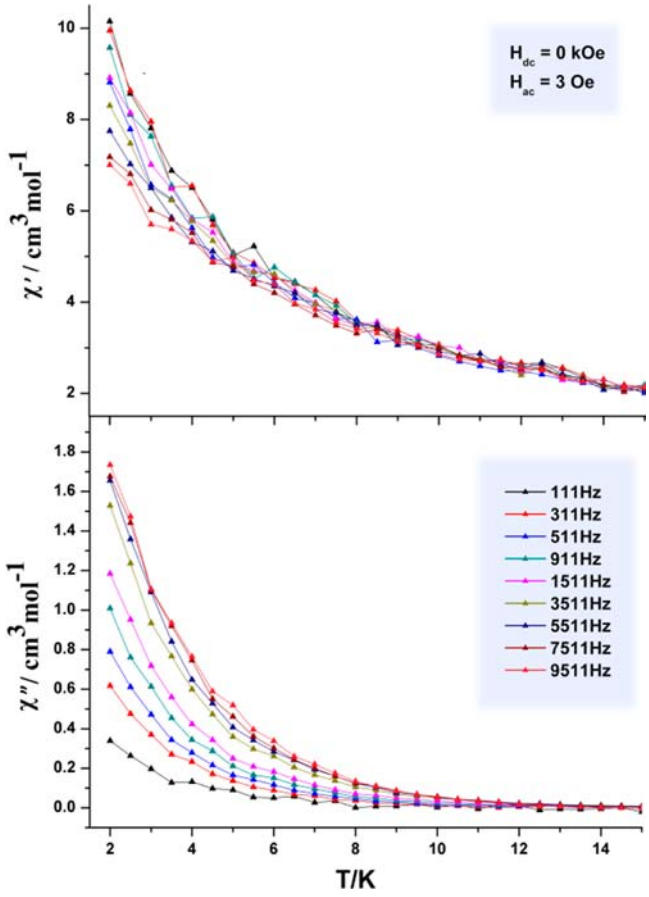

Figure 6. Plot of the in-phase (top) and out-of-phase (bottom) ac susceptibility for **3** in a zero dc field and a 3 Oe ac field.

21.53, and 22.48 Nβ, respectively (Supporting Information, Figures S4−S7). The saturation value of **1** is exactly equal to the expected value (21 Nβ for three Gd^{III} ions), while the saturation values of **2**−**4** are lower than the saturation sum values (27, 30, and 30 Nβ for three Tb^{III}, Dy^{III}, and Ho^{III} ions). The deviation from the expected magnetization saturation values of **2**−**4** reveals a strong ligand-field contribution, the presence of magnetic anisotropy, and/or low-lying excited states. Furthermore, the plots of the M versus H/T for complexes **2**−**4** show that the curves are not superimposed, which further confirm the presence of magnetic anisotropy (Supporting Information, Figures S8−S10). In addition, no obvious hysteresis loop is observed for all four complexes (Supporting Information, Figures S4−S7).

CONCLUSION

In conclusion, four isostructural heterometallic complexes **1**−**4** supported by thiacalix[4]arene have been successfully synthesized and structurally characterized. Structural analyses reveal that complexes **1**−**4** are stacked by some bent sandwich-like units constructed by two tail-to-tail calixarene molecules and an in between kite-like tetragonal (μ_4-OH) $Zn^{II}Ln^{III}_3$ cluster. And the sandwich-like entities further assemble into a slightly skewed head-to-head arrangement. The photoluminescent analyses show that the $BTC4A^{4-}$ ligands exhibit a good antenna effect for Tb^{3+} ions in complex **2**, and the ligand-to-lanthanide energy transfer process is effective for **2**. The magnetic properties of complexes **1**−**4** are examined, indicating some antiferromagnetic interactions between the Ln^{III} ions. In

dx.doi.org/10.1021/ic302367q | Inorg. Chem. 2013, 52, 3780−3786

addition, *ac* susceptibility measurement on **3** reveals an obvious frequency-dependent in- and out-of-phase signal, indicating slow magnetization relaxation typical for single-molecule magnets. This work provides another valuable approach to the design of polynuclear transition-lanthanide heterometallic materials using thiacalixarenes which might lead to some interesting luminescent and magnetic properties. Our efforts to prepare the new heterometallic complexes with multifunctional materials are ongoing.

■ ASSOCIATED CONTENT

Supporting Information

Crystallographic data of complexes **1**−**4** in CIF format. Plots of the in-phase and out-of phase ac susceptibility, TGA analyses, and PXRD patterns for **1**−**4**, and other materials. This material is available free of charge via the Internet at http://pubs.acs.org.

■ AUTHOR INFORMATION

Corresponding Author

*Phone: +86 591 83792460. Fax: +86 591 83714946. E-mail: hmc@fjirsm.ac.cn.

Notes

The authors declare no competing financial interest.

■ ACKNOWLEDGMENTS

We thank 973 Program (2011CBA00507; 2011CB932504), National Natural Foundation of China (21131006) and the Natural Science Foundation of Fujian Province for funding this research.

■ REFERENCES

(1) (a) Mereacre, V. M.; Ako, A. M.; Clerac, R.; Wernsdorfer, W.; Filoti, G.; Bartolome, J.; Anson, C. E.; Powell, A. K. *J. Am. Chem. Soc.* **2007**, *129*, 9248. (b) Kong, X. J.; Ren, Y. P.; Chen, W. X.; Long, L. S.; Zheng, Z. P.; Huang, R. B.; Zheng, L. S. *Angew. Chem., Int. Ed.* **2008**, *47*, 2398−2401. (c) Peng, J. B.; Zhang, Q. C.; Kong, X. J.; Zheng, Y. Z.; Ren, Y. P.; Long, L. S.; Huang, R. B.; Zheng, L. S.; Zheng, Z. P. *J. Am. Chem. Soc.* **2012**, *134*, 3314−3317.

(2) Li, C. J.; Lin, Z. J.; Peng, M. X.; Leng, J. D.; Yang, M. M.; Tong, M. L. *Chem. Commun.* **2008**, 6348−6350.

(3) Shibasaki, M.; Matsunaga, S.; Kumagai, N. *Synlett* **2008**, 1583−1602.

(4) (a) Papatriantafyllopoulou, C.; Wernsdorfer, W.; Abboud, K. A.; Christou, G. *Inorg. Chem.* **2011**, *50*, 421. (b) Zeng, Y. F.; Xu, G. C.; Hu, X.; Chen, Z.; Bu, X. H.; Gao, S.; Sanudo, E. C. *Inorg. Chem.* **2010**, *49*, 9734. (c) Karotsis, G.; Teat, S. J.; Wernsdorfer, W.; Piligkos, S.; Dalgarno, S. J.; Brechin, E. K. *Angew. Chem., Int. Ed.* **2009**, *48*, 8285−8288. (d) Visinescu, D.; Madalan, A. M.; Andruh, M.; Duhayon, C.; Sutter, J.-P.; Ungur, L.; Van den Heuvel, W.; Chibotaru, L. F. *Chem.—Eur. J.* **2009**, *15*, 11808. (e) Manoli, M.; Collins, A.; Parsons, S.; Candini, A.; Evangelisti, M.; Brechin, E. K. *J. Am. Chem. Soc.* **2008**, *130*, 11129. (f) Karotsis, G.; Evangelisti, M.; Dalgarno, S. J.; Brechin, E. K. *Angew. Chem., Int. Ed.* **2009**, *48*, 9928−9931. (g) Karotsis, G.; Kennedy, S.; Teat, S. J.; Beavers, C. M.; Fowler, D. A.; Morales, J. J.; Evangelisti, M.; Dalgarno, S. J.; Brechin, E. K. *J. Am. Chem. Soc.* **2010**, *132*, 12983−12990. (h) Canaj, A. B.; Tzimopoulos, D. I.; Philippidis, A.; Kostakis, G. E.; Milios, C. J. *Inorg. Chem.* **2012**, *51*, 7451−7453.

(5) (a) Zhao, B.; Chen, X. Y.; Cheng, P.; Liao, D. Z.; Yan, S. P.; Jiang, Z. H. *J. Am. Chem. Soc.* **2004**, *126*, 15394−15395. (b) Wong, W. K.; Yang, X. P.; Jones, R. A.; Rivers, J. H.; Lynch, V.; Lo, W. K.; Xiao, D.; Oye, M. M.; Holmes, A. L. *Inorg. Chem.* **2006**, *45*, 4340−4345. (c) Pasatoiu, T. D.; Tiseanu, C.; Madalan, A. M.; Jurca, B.; Duhayon, C.; Sutter, J. P.; Andruh, M. *Inorg. Chem.* **2011**, *50*, 5879−5889. (d) Liang, L.; Peng, G.; Ma, L.; Sun, L.; Deng, H.; Li, H.; Li, W. S. *Cryst. Growth Des.* **2012**, *12*, 1151−1158.

(6) Kahn, O. *Molecular Magnetism*; VCH: New York, 1993.

(7) (a) Stamatatos, T. C.; Teat, S. J.; Wernsdorfer, W.; Christou, G. *Angew. Chem., Int. Ed.* **2009**, *48*, 521−524. (b) Li, M. Y.; Lan, Y. H.; Ako, A. M.; Wernsdorfer, W.; Anson, C. E.; Buth, G.; Powell, A. K.; Wang, Z. M.; Gao, S. *Inorg. Chem.* **2010**, *49*, 11587−11594. (c) Abbas, G.; Lan, Y. H.; Mereacre, V.; Wernsdorfer, W.; Clerac, R.; Buth, G.; Sougrati, M. T.; Grandjean, F.; Long, G. J.; Anson, C. E.; Powell, A. K. *Inorg. Chem.* **2009**, *48*, 9345−9355. (d) Liu, Y.; Chen, Z.; Ren, J.; Zhao, X. Q.; Cheng, P.; Zhao, B. *Inorg. Chem.* **2012**, *51*, 7433−7435. (e) Colacio, E.; Ruiz, J.; Mota, A. J.; Palacios, M. A.; Cremades, E.; Ruiz, E.; White, F. J.; Brechin, E. K. *Inorg. Chem.* **2012**, *51*, 5857−5868. (f) Novitchi, G.; Pilet, G.; Ungur, L.; Moshchalkov, V. V.; Wernsdorfer, W.; Chibotaru, L. F.; Luneau, D.; Powell, A. K. *Chem. Sci.* **2012**, *3*, 1169−1176. (g) Leng, J. D.; Liu, J. L.; Tong, M. L. *Chem. Commun.* **2012**, *48*, 5286−5288. (h) Yamashita, A.; Watanabe, A.; Akine, S.; Nabeshima, T.; Nakano, M.; Yamamura, T.; Kajiwara, T. *Angew. Chem., Int. Ed.* **2011**, *50*, 4016−4019. (i) Akine, S.; Taniguchi, T.; Nabeshima, T. *Angew. Chem., Int. Ed.* **2002**, *41*, 4670−4673.

(8) (a) Guillemot, G.; Castellano, B.; Prange, T.; Solari, E.; Floriani, C. *Inorg. Chem.* **2007**, *46*, 5152−5154. (b) Aronica, C.; Chastanet, G.; Zueva, E.; Borshch, S. A.; Clemente-Juan, J. M.; Luneau, D. *J. Am. Chem. Soc.* **2008**, *130*, 2365−2371. (c) Karotsis, G.; Kennedy, S.; Dalgarno, S. J.; Brechin, E. K. *Chem. Commun.* **2010**, *46*, 3884−3886. (d) Taylor, S. M.; Karotsis, G.; McIntosh, R. D.; Kennedy, S.; Teat, S. J.; Beavers, C. M.; Wernsdorfer, W.; Piligkos, S.; Dalgarno, S. J.; Brechin, E. K. *Chem.—Eur. J.* **2011**, *17*, 7521−7530. (e) Sanz, S.; McIntosh, R. D.; Beavers, C. M.; Teat, S. J.; Evangelisti, M.; Brechin, E. K.; Dalgarno, S. J. *Chem. Commun.* **2012**, *48*, 1449−1451. (f) Liu, M.; Liao, W.; Hu, C.; Du, S.; Zhang, H. *Angew. Chem., Int. Ed.* **2012**, *51*, 1585−1588.

(9) (a) Kajiwara, T.; Iki, N.; Yamashita, M. *Coord. Chem. Rev.* **2007**, *251*, 1734−1746 , and references cited therein. (b) Dalgarno, S. J.; Claudio-Bosque, K. M.; Warren, J. E.; Glass, T. E.; Atwood, J. L. *Chem. Commun.* **2008**, 1410−1412. (c) Zeller, J.; Radius, U. *Inorg. Chem.* **2006**, *45*, 9487−9492.

(10) (a) Xiong, K. C.; Jiang, F. L.; Gai, Y. L.; He, Z. Z.; Yuan, D. Q.; Chen, L.; Su, K. Z.; Hong, M. C. *Cryst.Growth Des.* **2012**, *12*, 3335−3341. (b) Xiong, K. C.; Jiang, F. L.; Gai, Y. L.; Yuan, D. Q.; Chen, L.; Wu, M. Y.; Su, K. Z.; Hong, M. C. *Chem. Sci.* **2012**, *3*, 2321−2325. (c) Xiong, K. C.; Jiang, F. L.; Gai, Y. L.; Yuan, D. Q.; Han, D.; Ma, J.; Zhang, S. Q.; Hong, M. C. *Chem.—Eur. J.* **2012**, *18*, 5536−5540. (d) Xiong, K. C.; Jiang, F. L.; Gai, Y. L.; Zhou, Y. F.; Yuan, D. Q.; Su, K. Z.; Wang, X. Y.; Hong, M. C. *Inorg. Chem.* **2012**, *51*, 3283−3288. (e) Bi, Y. F.; Wang, X. T.; Liao, W. P.; Wang, X. F.; Wang, X. W.; Zhang, H. J.; Gao, S. *J. Am. Chem. Soc.* **2009**, *131*, 11650−11651. (f) Bi, Y. F.; Xu, G. C.; Liao, W. P.; Du, S. C.; Wang, X. W.; Deng, R. P.; Zhang, H. J.; Gao, S. *Chem. Commun.* **2010**, *46*, 6362−6364. (g) Bi, Y. F. B. Y. F.; Liao, W. P.; Wang, X. F.; Wang, X. W.; Zhang, H. J. *Dalton Trans.* **2011**, *40*, 1849−1851. (h) Liu, C.-M.; Zhang, D.-Q.; Hao, X.; Zhu, D.-B. *Chem.—Eur. J.* **2011**, *17*, 12285−12288.

(11) (a) Bi, Y. F.; Wang, X. T.; Liao, W. P.; Wang, X. W.; Deng, R. P.; Zhang, H. J.; Gao, S. *Inorg. Chem.* **2009**, *48*, 11743−11747. (b) Fairbairn, R. E.; McLellan, R.; McIntosh, R. D.; Taylor, S. M.; Brechin, E. K.; Dalgarno, S. J. *Chem. Commun.* **2012**, *48*, 8493−8495.

(12) (a) Kajiwara, T.; Wu, H. S.; Ito, T.; Iki, N.; Miyano, S. *Angew. Chem., Int. Ed.* **2004**, *43*, 1832−1835. (b) Kajiwara, T.; Katagiri, K.; Hasegawa, M.; Ishii, A.; Ferbinteanu, M.; Takaishi, S.; Ito, T.; Yamashita, M.; Iki, N. *Inorg. Chem.* **2006**, *45*, 4880−4882. (c) Kajiwara, T.; Katagiri, K.; Takaishi, S.; Yamashita, M.; Iki, N. *Chem.—Asian J.* **2006**, *1*, 349−351. (d) Bi, Y. F.; Du, S. C.; Liao, W. P. *Chem. Commun.* **2011**, *47*, 4724−4726. (e) Liu, C. M.; Zhang, D. Q.; Hao, X.; Zhu, D. B. *Cryst.Growth Des.* **2012**, *12*, 2948−2954. (f) Dai, F. R.; Wang, Z. Q. *J. Am. Chem. Soc.* **2012**, *134*, 8002−8005. (g) Du, S.; Hu, C.; Xiao, J.-C.; Tan, H.; Liao, W. *Chem. Commun.* **2012**, *48*, 9177−9179.

(13) (a) Xiong, K. C.; Wang, X. Y.; Jiang, F. L.; Gai, Y. L.; Xu, W. T.; Su, K. Z.; Li, X. J.; Yuan, D. Q.; Hong, M. C. *Chem. Commun.* **2012**, *48*, 7456−7458. (b) Sanz, S.; Ferreira, K.; McIntosh, R. D.; Dalgarno, S. J.; Brechin, E. K. *Chem. Commun.* **2011**, *47*, 9042−9044. (c) Bi, Y. F.; Li, Y. L.; Liao, W. P.; Zhang, H. J.; Li, D. Q. *Inorg. Chem.* **2008**, *47*,

9733−9735. (d) Bi, Y. F.; Wang, X. T.; Wang, B. W.; Liao, W. P.; Wang, X. F.; Zhang, H. J.; Gao, S.; Li, D. Q. *Dalton Trans.* **2009**, 2250−2254.
(14) (a) Iki, N.; Kabuto, C.; Fukushima, T.; Kumagai, H.; Takeya, H.; Miyanari, S.; Miyashi, T.; Miyano, S. *Tetrahedron* **2000**, *56*, 1437−1443. (b) Lhotak, P.; Smejkal, T.; Stibor, I.; Havlicek, J.; Tkadlecova, M.; Petrickova, H. *Tetrahedron Lett.* **2003**, *44*, 8093−8097.
(15) *CrystalClear*, Version 1.3.6; Rigaku/MSC: The Woodlands, TX, 2004
(16) (a) Sheldrick, G. M. *PSHELXS 97, Program for crystal Structure Solution*; University of Göttingen: Göttingen, Germany, 1997. (b) Sheldrick, G. M. *SHELXL 97, Program for crystal Structure Refinement*; University of Göttingen: Göttingen, Germany, 1997.
(17) Long, J.; Habib, F.; Lin, P.-H.; Korobkov, I.; Enright, G.; Ungur, L.; Wernsdorfer, W.; Chibotaru, L. F.; Murugesu, M. *J. Am. Chem. Soc.* **2011**, *133*, 5319.
(18) (a) Kahn, M. L.; Ballou, R.; Porcher, P.; Kahn, O.; Sutter, J. P. *Chem.—Eur. J.* **2002**, *8*, 525−531. (b) Abbas, G.; Lan, Y. H.; Kostakis, G. E.; Wernsdorfer, W.; Anson, C. E.; Powell, A. K. *Inorg. Chem.* **2010**, *49*, 8067−8072. (c) Majeed, Z.; Mondal, K. C.; Kostakis, G. E.; Lan, Y. H.; Anson, C. E.; Powell, A. K. *Chem. Commun.* **2010**, *46*, 2551−2553.